

Binding characteristics and sensitivity to endogenous dopamine of [¹¹C]-(+)-PHNO, a new agonist radiotracer for imaging the high-affinity state of D₂ receptors *in vivo* using positron emission tomography

Nathalie Ginovart,*† Laurent Galineau,* Matthaeus Willeit,* Romina Mizrahi,* Peter M. Bloomfield,* Philip Seeman,‡ Sylvain Houle,*† Shitij Kapur*† and Alan A. Wilson*†

*The Vivian Rakoff Positron Emission Tomography Unit, Center for Addiction and Mental Health, Toronto, Canada

†Department of Psychiatry, University of Toronto, Canada

‡Department of Pharmacology, University of Toronto, Canada

Abstract

[¹¹C]-(+)-PHNO (4-propyl-9-hydroxynaphthoxazine) is a new agonist radioligand that provides a unique opportunity to measure the high-affinity states of the D₂ receptors (D₂-high) using positron emission tomography (PET). Here we report on the distribution, displaceability, specificity and modeling of [¹¹C]-(+)-PHNO and compare it with the well characterized antagonist D₂ radioligand, [¹¹C]raclopride, in cat. [¹¹C]-(+)-PHNO displayed high uptake in striatum with a mean striatal binding potential (BP) of 3.95 ± 0.85. Pre-treatment with specific D₁ (SCH23390), D₂ (raclopride, haloperidol) and D₃ receptor (SB-277011) antagonists indicated that [¹¹C]-(+)-PHNO binding in striatum is specific to D₂ receptors. Within-subject comparisons showed that [¹¹C]-(+)-PHNO BP in striatum was almost 2.5-fold higher than that measured with [¹¹C]-(-)-NPA ([¹¹C]-(-)-N-propyl-norapomorphine). Compar-

ison of the dose-effect of amphetamine (0.1, 0.5 and 2 mg/kg; i.v.) showed that [¹¹C]-(+)-PHNO was more sensitive to the dopamine releasing effect of amphetamine than [¹¹C]raclopride. Amphetamine induced up to 83 ± 4% inhibition of [¹¹C]-(+)-PHNO BP and only up to 56 ± 8% inhibition of [¹¹C]raclopride BP. Scatchard analyses of [¹¹C]-(+)-PHNO and [¹¹C]raclopride bindings in two cats showed that the B_{max} obtained with the agonist (29.6 and 32.9 pmol/mL) equalled that obtained with the antagonist (30.6 and 33.4 pmol/mL). The high penetration of [¹¹C]-(+)-PHNO in brain, its high signal-to-noise ratio, its favorable *in vivo* kinetics and its high sensitivity to amphetamine shows that [¹¹C]-(+)-PHNO has highly suitable characteristics for probing the D₂-high with PET.

Keywords: D₂ receptors, d-amphetamine, dopamine, naphthoxazine derivatives, raclopride.

J. Neurochem. (2006) **97**, 1089–1103.

Dopamine (DA) has been implicated in a variety of physiological functions and dysfunctions that are involved in several disorders, including Parkinson's disease and schizophrenia (Carlsson 1987; Zigmond *et al.* 1990). DA exerts its pharmacological action through multiple membrane-spanning proteins of the G protein-coupled receptor (GPCR) superfamily. These may be divided into two subfamilies of receptor subtypes based on their structures, their linkage to adenylate cyclase and their pharmacological properties: the D₁-like (D₁, D₅) and the D₂-like receptor subtypes (D₂, D₃, D₄; Strange 1993). In the D₂ subfamily, the D₂ receptor subtype appears central to the pathology of schizophrenia, tardive dyskinesia,

Received November 22, 2005; revised manuscript received January 25, 2006; accepted January 25, 2006.

Address correspondence and reprint requests to Nathalie Ginovart, PET Center, CAMH, 250 College Street, Toronto, Ontario, M5T 1R8, Canada. E-mail: nathalie.ginovart@camhpet.ca

Abbreviations used: B_{max}, binding site density; BP, binding potential; 2D, two-dimensional; 3D, three-dimensional; D₂-high, high-affinity states of the D₂ receptors; D₂-low, low-affinity states of the D₂ receptors; DA, dopamine; ETCO₂, end-tidal carbon dioxide pressure; GPCR, G protein-coupled receptor; K'_D, apparent equilibrium dissociation constant; NPA, N-propyl-norapomorphine; PET, positron emission tomography; PHNO, 4-propyl-9-hydroxynaphthoxazine; RM ANOVA, ANOVA with repeated measures; SR, specific radioactivity; SUV, standard uptake values.

Parkinson's disease and drug addiction. Like many other GPCRs, D₂ receptors have been shown to exist in two interconvertible affinity states: a state of high affinity (denoted as D₂-high) and a state of low affinity (denoted as D₂-low) for their naturally occurring agonist DA (Sibley *et al.* 1982). The D₂-high represents the active form of the receptor that is coupled to the G protein and capable of inhibiting adenylate cyclase (Zahniser and Molinoff 1978). The D₂-high is regulated by guanine nucleotides and is convertible into the D₂-low, which corresponds to the inactive, G protein-uncoupled form of the receptor.

Unlike agonists, which preferentially bind to the D₂-high, antagonists recognize D₂-high and D₂-low with equal affinity (George *et al.* 1985). Thus, studies of D₂ receptors using antagonist radioligands cannot distinguish pathological states that reflect a shift in the proportion of D₂-high and D₂-low. This might be particularly true for pathologies such as schizophrenia, for which an increased density of striatal D₂ receptors has been suspected to account for the DA hyperfunction seen in this disease, but has generally not been confirmed by brain imaging studies using D₂ antagonist radiotracers (Farde *et al.* 1990; Martinot *et al.* 1990, 1991; Hietala *et al.* 1994; Nordstrom *et al.* 1995). Recent studies using positron emission tomography (PET), or single photon emitted computed tomography, and high affinity D₂/D₃ radiotracers, in fact provided evidence of a decreased density of D₂ receptors in extrastriatal brain regions such as temporal cortex (Tuppurainen *et al.* 2003), anterior cingulate (Suhara *et al.* 2002) and thalamus (Talvik *et al.* 2003; Yasuno *et al.* 2004) in patients with schizophrenia when compared with healthy controls.

In recent years, there have been multiple efforts to develop agonist radiotracers for *in vivo* imaging of the D₂-high using PET. A number of ¹¹C- or ¹⁸F-labeled derivatives of apomorphine (Halldin *et al.* 1992; Zijlstra *et al.* 1993a,b; Hwang *et al.* 2000; Finnema *et al.* 2005) and hydroxytetralin (Shi *et al.* 1999; Mukherjee *et al.* 2000, 2004; Shi *et al.* 2004) with nanomolar affinities for D₂ receptors have been reported as potential agonist PET radioligands. The most promising agonist radiotracer reported so far, [¹¹C]N-(–)-propyl-norapomorphine {[¹¹C]-(–)-NPA}, shows a striatum/cerebellum ratio of 2.8 *in vivo* in baboon (Hwang *et al.* 2000). As expected for an agonist radioligand, [¹¹C]-(–)-NPA shows an increased sensitivity to amphetamine-released DA when compared with [¹¹C]raclopride in anesthetized baboons (Narendran *et al.* 2004). Although the striatum/cerebellum ratio obtained in baboon with [¹¹C]-(–)-NPA was the highest reported so far with a D₂ agonist, its binding potential (BP) (denoted as 'V₃' in Narendran *et al.* 2004) of 1.2 in baboon is only about 40% of the value of the BP of [¹¹C]raclopride obtained in the same animals. The use of [¹¹C]-(–)-NPA has not yet been reported in humans. However, its rather modest signal-to-noise ratio may weaken the power of [¹¹C]-(–)-NPA PET imaging in human trials.

In 1984, a series of naphthoxazine derivatives was described, with a molecular structure unrelated to apomorphine, which showed a high *in vitro* affinity and *in vivo* agonistic activity at the D₂ receptors (Horn *et al.* 1984; Jones *et al.* 1984). One member of this series, the (+)-enantiomer of 4-propyl-3,4,4a,5,6,10b-hexahydro-2H-naphtho[1,2-b][1,4]oxazin-9-ol] {(+)-PHNO}, was shown to be a remarkably potent and selective D₂ agonist both *in vivo* and *in vitro*. *In vivo* functional assays of D₂ receptors demonstrated that (+)-PHNO was able to induce hypothermia and postural asymmetry in mice with unilateral lesion of the striatum, stereotypies in rats, contralateral turning in rats with unilateral lesion of the substantia nigra, emesis in beagles and inhibition of the firing of nigral dopaminergic neurons with ED₅₀ values ranging between 0.5 and 13 µg/kg intraperitoneally (Martin *et al.* 1984, 1985). Receptor binding assays showed that (+)-PHNO displayed high affinity and selectivity for the D₂ receptor, with an equilibrium dissociation constant of 0.3–0.6 nmol/L at the D₂-high, and >100-fold less at the D₂-low (Madras *et al.* 1988; Seeman and Ulpian 1988; Seeman *et al.* 1993). Most importantly, the non-hydrolysable guanine nucleotide, guanylyl-5'-imidodiphosphate Gpp(NH)p (a stable analog of GTP), inhibited [³H]-(+)-PHNO specific binding in canine striatal homogenates (Seeman *et al.* 1993) and on rat striatal sections (Nobrega and Seeman 1994), providing direct evidence that [³H]-(+)-PHNO binds primarily to the D₂-high. We recently radiolabeled (+)-PHNO with ¹¹C and obtained *ex vivo* data in rats showing that [¹¹C]-(+)-PHNO is a promising agonist radiotracer for *in vivo* labeling of the D₂-high (Wilson *et al.* 2005). *Ex vivo* binding of [¹¹C]-(+)-PHNO in striatum was found to be stereospecific, saturable, specific to the D₂ receptors, and to display appropriate sensitivity to variations in the levels of endogenous DA (Wilson *et al.* 2005). Moreover, [¹¹C]-(+)-PHNO displayed a higher striatum-to-cerebellum ratio when compared with [¹¹C]-(–)-NPA (5.6 and 4.3 at 60 min post-injection for [¹¹C]-(+)-PHNO and [¹¹C]-(–)-NPA, respectively), suggesting that [¹¹C]-(+)-PHNO could be a superior radioligand for imaging the D₂-high using PET (Wilson *et al.* 2005). Recent pilot data obtained using PET in healthy humans showed that [¹¹C]-(+)-PHNO binding displays favorable kinetics and allows an exquisite delineation of brain structures known to contain D₂/D₃ receptors (Gurevich and Joyce 1999) such as the caudate, the putamen, the external globus pallidus and the substantia nigra (Willeit *et al.* 2006).

In this study, *in vivo* PET experiments were performed in cats to allow investigations that were otherwise not possible in humans, especially experiments involving the use of doses of pharmacological compounds that lie above the doses acceptable in human beings. First, we report on the regional brain distribution and *in vivo* kinetics of [¹¹C]-(+)-PHNO binding, using PET, in the cat brain. For comparison, we also examined the *in vivo* kinetics of [¹¹C]-(–)-NPA binding and that of the

inactive enantiomer of (+)-PHNO, [¹¹C]-(-)-PHNO. A pharmacological characterization of [¹¹C]-(+)-PHNO binding was performed, using reference compounds known to be active at either the D₁, D₂ or D₃ receptors, to further validate [¹¹C]-(+)-PHNO as a novel agonist radiotracer for imaging the D₂-high using PET. Second, we describe the dose-effect of d-amphetamine and haloperidol on both [¹¹C]-(+)-PHNO and [¹¹C]raclopride binding in the same animals. Our hypothesis was that both d-amphetamine and haloperidol should induce a dose-dependent decrease in [¹¹C]-(+)-PHNO and [¹¹C]raclopride binding in striatum. However, as both endogenous DA and [¹¹C]-(+)-PHNO bind to the D₂-high, d-amphetamine should have a larger effect on [¹¹C]-(+)-PHNO than on [¹¹C]raclopride binding. Conversely, as haloperidol binds to both the D₂-high and D₂-low, haloperidol should have a similar effect on both radioligands. Third, pilot Scatchard analyses were performed in two cats to compare the binding properties, in terms of binding sites density and apparent affinity, of the D₂ receptor populations as labeled by [¹¹C]-(+)-PHNO and [¹¹C]raclopride.

Materials and methods

Animals

Animal studies and experimental procedures conformed to the guidelines established by the Canadian Council on Animal Care, and were approved by the Animal Care Committees at both the Center for Addiction and Mental Health and the University of Toronto. A total of five domestic male cats (Liberty Research Inc., Waverly, NY, USA) weighing 5–7 kg were used in this study.

PET system

Studies were performed using a high resolution neuro-PET camera system, CPS-HRRT (CPS Innovations, Knoxville, TN, USA), which measured radioactivity in 207 brain sections with a thickness of 1.2 mm each. This camera system consists of eight panel detectors, each panel being composed of 117 phoswich detectors, arranged 13 axial by 9 radial. The phoswich detector is manufactured from two different crystal materials, a lutetium oxyorthosilicate (LSO) crystal and a lutetium yttrium oxyorthosilicate (LYSO) crystal, each crystal element having a dimension of 2 × 2 × 10 mm³. The in-plane resolution of the scanner is approximately 2.8 mm full width at half-maximum. The HRRT acquires data in both 64-bit and 32-bit list mode formats under the control of the acquisition PC (SuperMicro Computer Inc., San Jose, CA, USA) computer. The major difference between the two list mode formats is that the former defines precisely the coincidence between the detector pair for each event, whilst the later converts the actual position of the coincidence in the sinogram space.

Image acquisition and reconstruction

Transmission scans, both blank and with the animal in the tomograph field of view, were acquired in 64-bit list mode using a single photon point source, ¹³⁷Cs (T_{1/2} = 30.2 years, E_γ = 662 keV). The acquired list mode data were sorted into sinograms

and an attenuation image calculated from the ratio of these two scans (Knoess *et al.* 2003). However, a further correction had to be applied to account for the difference in the photon energy between transmission [E_γ = 662 kilo-electronvolt (keV)] and emission (E_γ = 511 keV) acquisitions. A 511 keV attenuation image was generated by linearly re-scaling the 662 keV attenuation image prior to forward projection of the scaled 511 keV attenuation image to produce the attenuation correction. This re-scaling process also accounted globally for the scatter contamination in transmission data (Knoess *et al.* 2003).

Following the transmission acquisition, a 32-bit list mode emission acquisition of 65 min duration was initiated. The injection of the radioligand was started a few seconds after the start of the emission acquisition. On completion of the emission acquisition, both the transmission and emission data were transferred to an off-line data processing system for image reconstruction. The emission list mode data were re-binned into a series of three-dimensional (3D) sinograms. The first frame was of variable length to account for the time between the start of the acquisition and the arrival of radioactivity in the tomography field of view. The following 28 frames were then defined as 5 × 60 s frames, 20 × 2 min frames and 3 × 5 min frames. For each 3D sinogram, the following processes were completed to create a reconstructed image. First, the gaps in the sinogram due to the design of the tomography were filled (Karp *et al.* 1988), during which process corrections for photon attenuation and detector normalization were applied. The gap-filled sinograms were scatter-corrected (Watson *et al.* 1997) before applying Fourier re-binning to convert the 3D sinograms into two-dimensional (2D) sinograms (Defrise *et al.* 1997). The 2D sinograms were then reconstructed into image space, using a 2D filtered back projection algorithm with a ramp filter at Nyquist cut-off frequency, and the images calibrated to nCi/cc. When all the frames had been reconstructed, the images were combined to create a single dynamic data set upon which time-activity curves were calculated.

Radiochemistry

[¹¹C]-(+)-PHNO and [¹¹C]-(-)-PHNO were synthesized as previously described (Wilson *et al.* 2005). [¹¹C]-(-)-NPA was prepared in a similar manner to [¹¹C]-(+)-PHNO, using normethylapomorphine hydrochloride (Sigma-Aldrich, Oakville, Ontario, Canada) as precursor. [¹¹C]raclopride was synthesized as previously described by methylation of the desmethyl precursor (free base) using [¹¹C]methyl iodide (Ehrin *et al.* 1987; Wilson *et al.* 2000). For all radiotracers, radiochemical purity was > 98%.

PET examinations

Anesthesia was induced with isoflurane (4%). As soon as deep anesthesia was obtained, an endotracheal intubation was performed and anesthesia was maintained by constant insufflation of 2.5% isoflurane in oxygen. End-tidal carbon dioxide pressure (ETCO₂), heart rhythm and body temperature were continuously monitored during the PET experiments. Ventilation was assisted using an ADS 1000 microprocessor-controlled ventilator (Engler Engineering, Hialeah, FL, USA). Standard ventilation parameters (flow rate: 10–12 L/min; 8–10 breaths/min; peak inspiratory pressure: 14–16 cm/H₂O) were used. During the experiment, ventilation was modified within the above standard values to target ETCO₂ values of 28–31 mmHg. A head fixation system was used to secure

a reproducible position of the cat's head during the PET measurements. This system consists of a stereotaxic frame similar to frames used for standard cat surgical stereotactic procedures, except that it is constructed with plexiglas to reduce the attenuation and scatter of photons during PET scans. For positioning of the cat into the frame, ear bars were inserted into the external auditory meatus of the animal to orient its interaural line. A tooth bar and orbital bars were used to place the animal's head in the orientation defined in the cat atlas of Jasper and Ajmone-Marsan (1954). The frame was attached directly to the computer-controlled bed of the PET scanner so that the animal could be precisely placed in the same axial position of the scanner field of view. A cannula was inserted into the recurrent tarsal vein on the lateral aspect of the hind limb for radiotracer injection.

PET experiments were performed after an i.v. bolus injection of either [^{11}C]-(+)-PHNO, [^{11}C]-(-)-PHNO, [^{11}C]-(-)-NPA or [^{11}C]raclopride. For [^{11}C]-(+)-PHNO, 2.3 ± 0.2 mCi of the radioligand was injected at a specific radioactivity (SR) of 993 ± 386 Ci/mmol at the time of i.v. injection. For [^{11}C]-(-)-PHNO, 2.3 mCi of the radioligand was injected at a SR of 982 and 1196 Ci/mmol. For [^{11}C]-(-)-NPA, 2.1 ± 0.3 mCi of the radioligand was injected at a SR of 1249 ± 490 Ci/mmol. For [^{11}C]raclopride, 2.4 ± 0.2 mCi of the radioligand was injected at a SR of 1042 ± 298 Ci/mmol. For each radioligand, the total time for radioactivity measurement was 60 min.

***In vivo* characterization of [^{11}C]-(+)-PHNO binding in the cat brain**

Three cats were each examined with [^{11}C]-(+)-PHNO in two consecutive PET experiments performed 2.25 h apart. The first PET experiment was performed at baseline conditions in order to obtain information about the regional distribution and the kinetics of [^{11}C]-(+)-PHNO in brain. The second experiment was performed following a pre-treatment with either the D_2 receptor antagonist, raclopride (1 mg/kg; i.v.), the D_2 receptor antagonist, haloperidol (0.5 mg/kg; i.v.), the D_1 receptor antagonist, SCH23390 (1 mg/kg; i.v.), or the D_3 receptor antagonist, SB-277011 (1 mg/kg; i.v.). Raclopride, SCH23390 and SB-277011 were administered 15 min prior to, while haloperidol was administered 1 h prior to the [^{11}C]-(+)-PHNO injection.

Comparison of [^{11}C]-(+)-PHNO and [^{11}C]-(-)-NPA *in vivo* binding kinetics

Two cats were sequentially examined, at baseline conditions, following administration of [^{11}C]-(+)-PHNO and [^{11}C]-(-)-NPA. The time interval between the [^{11}C]-(+)-PHNO and [^{11}C]-(-)-NPA scans was at least 1 month.

Effect of amphetamine on [^{11}C]-(+)-PHNO, [^{11}C]-(-)-PHNO and [^{11}C]-(-)-NPA bindings

One cat was examined on four different experimental days. On the first experimental day, the cat was scanned using [^{11}C]-(+)-PHNO at baseline conditions and at 20 min following a single administration of d-amphetamine (2 mg/kg; i.v.). On the second experimental day, the same cat was scanned using the inactive enantiomer [^{11}C]-(-)-PHNO at baseline conditions and at 20 min following a single administration of d-amphetamine (2 mg/kg; i.v.). The time interval between the first and second experimental day was 5 months. On the

third experimental day, the cat was scanned using [^{11}C]-(+)-PHNO at 1 h and at 3.5 h following a single administration of d-amphetamine (2 mg/kg; i.v.). The time interval between the second and third experimental day was 2 weeks. On the fourth experimental day, the cat was scanned using [^{11}C]-(-)-NPA at baseline conditions and at 20 min following an administration of d-amphetamine (2 mg/kg; i.v.). The time interval between the third and fourth experimental day was 10 months.

Dose-effect of d-amphetamine on [^{11}C]-(+)-PHNO and [^{11}C]raclopride binding

Five cats were used, for a total of 28 PET scans, to compare the dose-effect of d-amphetamine on [^{11}C]-(+)-PHNO and [^{11}C]raclopride binding. These 28 scans were performed in 14 experimental days, seven using [^{11}C]-(+)-PHNO and seven using [^{11}C]raclopride. On each experimental day, cats participated in two consecutive PET scans performed 2–2.25 h apart. The first scan was performed at baseline conditions and the second scan was performed at 20 min after a single i.v. administration of d-amphetamine. Three doses of d-amphetamine were used: 0.1 mg/kg ($n = 2$), 0.5 mg/kg ($n = 2$) and 2 mg/kg ($n = 3$). Cats were randomly assigned to one or two doses of d-amphetamine: three cats were tested with one dose and two cats with two doses of d-amphetamine. However, each animal was tested with the same d-amphetamine dose(s) for both [^{11}C]-(+)-PHNO and [^{11}C]raclopride, and the sequence of radioligand injection was counterbalanced.

Dose-effect of haloperidol on [^{11}C]-(+)-PHNO and [^{11}C]raclopride binding

Four cats were used, for a total of 16 PET scans, to compare the dose-effect of haloperidol on [^{11}C]-(+)-PHNO and [^{11}C]raclopride binding. Ten scans were performed using [^{11}C]-(+)-PHNO and were acquired on 4 experimental days. On each experimental day, cats participated in two consecutive PET scans performed 2.2 h apart. The first scan was performed at baseline conditions and the second scan was performed 20 min after a single i.v. administration of haloperidol. Three doses of haloperidol were tested in three different cats: 0.002 mg/kg, 0.005 mg/kg and 0.5 mg/kg. Two additional PET scans (baseline and post-haloperidol) were performed in a fourth cat to re-test the effect of a 0.002 mg/kg dose of haloperidol. Six scans were performed using [^{11}C]raclopride in a manner similar to that described with [^{11}C]-(+)-PHNO except in that case, we did not repeat the experiments using the 0.002 mg/kg dose of haloperidol in a fourth cat. Each animal was tested with the same dose of haloperidol for both [^{11}C]-(+)-PHNO and [^{11}C]raclopride and the sequence of radioligand injection was counterbalanced.

Scatchard analyses of [^{11}C]-(+)-PHNO and [^{11}C]raclopride bindings

Two cats (cat C and cat E) were each examined on two occasions, at least one week apart. [^{11}C]-(+)-PHNO was used on one occasion and [^{11}C]raclopride on the other. On each occasion, cats were examined at baseline conditions in two consecutive PET experiments, performed 2 h apart, using the radioligand at high (> 600 Ci/mmol) and low specific radioactivity (SR; approximately 40 Ci/mmol), respectively. In the high SR experiments, the masses of raclopride injected were 0.14 $\mu\text{g}/\text{kg}$ and 0.10 $\mu\text{g}/\text{kg}$ of body weight in cats C and E, respectively; the masses of (+)-PHNO were

0.13 µg/kg and 0.13 µg/kg of body weight in the two corresponding cats, respectively. In the low SR experiments, the masses of raclopride injected were 4.83 µg/kg and 6.60 µg/kg of body weight in cats C and E, respectively; the masses of (+)-PHNO were 1.85 µg/kg and 2.52 µg/kg of body weight in the two corresponding cats, respectively. On each occasion, the radioligand binding site density (B_{\max}) and apparent equilibrium dissociation constant (K'_D) were calculated by Scatchard analysis.

Data analysis

Regions of interest analysis

The stereotaxic frame used in this study enables a reproducible positioning of the cat's head within the scanner field of view and allows for the same regions of interest (ROIs) to be used across serial studies of a same animal. ROIs for the right and left striatum and the cerebellum were drawn on summation PET images obtained with [¹¹C]-(+)-PHNO at baseline conditions. The summation images used represented radioactivity accumulation from 10 to 60 min post-radioligand injection. ROIs for the striatum included the caudate and the putamen, and were defined on the four central PET slices where the caudate-putamen had its maximal extension. For each cat, the same set of ROIs was used across studies and across radioligands. When analyzing serial scans of a same animal, inspection of the ROIs positioning was systematically carried out and found to be in close agreement across studies. ROIs were then transferred onto the dynamic PET images, and regional radioactivity concentration (nCi/mL) was determined for each frame, corrected for decay and expressed as standardized uptake value (SUV) according to the equation (Bergstrom *et al.* 2003):

$$\text{SUV} = \frac{\text{regional radioactivity concentration}}{\text{(injected radioactivity/body weight)}}$$

Time-activity curves for regional radioligand uptake were generated by plotting SUV values versus time.

Binding potential quantification

Quantification of radioligand binding potentials (BP) was performed using the ratio method. The time-activity curve for specific radioligand binding, $C_B(t)$, was defined as the radioactivity concentration in a ROI minus that measured in the cerebellum: $C_B(t) = C_{\text{ROI}}(t) - C_{\text{CEREB}}(t)$. Radioactivity in the cerebellum was thus used as an estimate for free and non-specific concentration of radioactivity in brain, $C_{\text{NS+F}}$. The time-curves for C_B and $C_{\text{NS+F}}$ were integrated from $t_1 = 31$ min to $t_2 = 60$ min. The BP was calculated as the ratio between the integrated value obtained for C_B and the integrated value obtained for $C_{\text{NS+F}}$.

Drug-induced occupancy and dose-responses

Following pre-treatment with amphetamine and haloperidol, D_2 receptor occupancy in the striatum was defined as the percentage reduction of BP obtained after drug treatment compared with the BP obtained at baseline. The relationships between the injected doses (mg/kg) of d-amphetamine and haloperidol, and their respective brain-induced occupancy of D_2 receptors, were examined. According to the law of mass action, the relationship between receptor occupancy and drug dose is described by the hyperbolic function:

$$\text{Occupancy}(\%) = \frac{\text{Occ}_{\max} \times \text{Dose}}{\text{ED}_{50} + \text{Dose}} \quad (1)$$

where Occ_{\max} is the maximal occupancy induced by the drug, dose is the drug injected dose (mg/kg) and ED_{50} is the drug dose (mg/kg) inducing 50% of the Occ_{\max} .

The D_2 receptor occupancy values measured after injection of either d-amphetamine or haloperidol were plotted versus the corresponding drug injected doses. Each data point was treated as a separate observation. The hyperbolic function of eqn 1 was fitted to the experimental data points using an iterative weighted least squares technique implemented in KALEIDAGRAPH 4.0 Software (Synergy Software, Reading, PA, USA). ED_{50} (mg/kg) and Occ_{\max} (%) values were then extrapolated from the fitted curves.

Scatchard analyses

Scatchard analyses of [¹¹C]raclopride and [¹¹C]-(+)-PHNO bindings were performed as previously described (Farde *et al.* 1990). The time curve for radioactivity in cerebellum, a region with a low density of D_2 receptors, was used as an estimate of free and non-specific radioligand concentration in brain [$F(t)$]. The time curve for specific radioligand binding [$B(t)$] was defined as the radioactivity in the striatum minus that in the cerebellum. A set of three exponential functions was fitted to the time curves for $B(t)$ and $F(t)$. Time for transient equilibrium was defined as the moment when $B(t)$ peaked, i.e. $dB/dt = 0$. The B/F ratio was calculated using the values obtained at transient equilibrium. The value of B obtained at transient equilibrium was divided by the SR of injected [¹¹C]raclopride to obtain the specifically bound radioligand concentration (B; pmol/mL). The B/F ratios obtained for each experiment were plotted versus B in a Scatchard graph and a straight line was drawn through the plotted points. The B_{\max} was defined as the intercept with the x-axis and the K'_D by the inverse of the slope.

Statistical analysis

Differences in BPs, as well as occupancies between radioligands and between doses of d-amphetamine or haloperidol, were tested with repeated measures ANOVA (RM ANOVA). Omnibus tests were performed to evaluate the effect of radioligand and dose on BPs and occupancies following pre-treatment with either d-amphetamine or haloperidol. Bonferroni-corrected comparisons were used as post-hoc tests to evaluate significant differences between radioligands and between doses. Since interaction terms were not significant in all cases, they were removed from the models. We used ANOVA when different groups of cats were used between radioligands. All statistical tests are two-tailed and a $p < 0.05$ was set as statistically significant in all cases.

Results

In vivo characterization of [¹¹C]-(+)-PHNO binding in the cat brain

The *in vivo* distribution of [¹¹C]-(+)-PHNO binding was consistent with the known distribution of D_2 receptors in brain, with a high uptake of radioactivity observed in striatum and a low uptake of radioactivity observed in cerebellum. [¹¹C]-(+)-PHNO kinetics were fast, with the peak of radioactivity

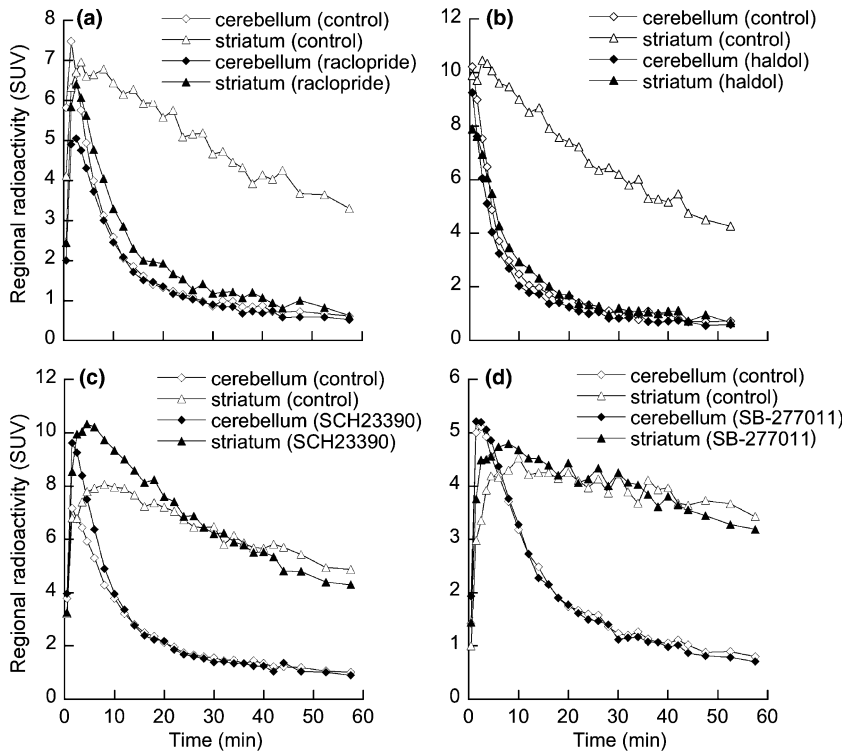


Fig. 1 Time–activity curves showing [^{11}C]-(+)-PHNO binding kinetics in striatum and cerebellum at control conditions and following pretreatment with (a) raclopride, (b) haloperidol, (c) SCH23390 and (d) SB-277011.

levels reached within 2 min and within 8–10 min post-injection in cerebellum and in striatum, respectively. [^{11}C]-(+)-PHNO specific binding in striatum was determined by subtracting the radioactivity measured in cerebellum from that measured in striatum. Striatal specific binding peaked at about 15–20 min post-injection and declined thereafter, indicating that [^{11}C]-(+)-PHNO binding in this structure is reversible and reaches equilibrium well within the time frame of a PET experiment. The mean [^{11}C]-(+)-PHNO BP, approximated using the ratio method and data obtained between 31 and 60 min post-injection, was 3.95 ± 0.85 ($n = 5$).

In pre-treatment experiments, [^{11}C]-(+)-PHNO binding was markedly reduced in striatum but not in cerebellum following injection of both raclopride (1 mg/kg; Fig. 1a) and haloperidol (0.5 mg/kg; Fig. 1b). Striatal BP was reduced by 89% and 94% following pre-treatment with raclopride and haloperidol, respectively. Pre-treatment with either SCH23390 (1 mg/kg; Fig. 1c) or SB-277011 (1 mg/kg; Fig. 1d) had no measurable effect on [^{11}C]-(+)-PHNO binding in either striatum or cerebellum.

Figure 2 shows a comparison of the baseline time–activity curves obtained in the same cat after administration of the active and inactive enantiomers of [^{11}C]-PHNO. The inactive enantiomer, [^{11}C]-(-)-PHNO, showed no preferential uptake in striatum when compared with cerebellum, with a BP of 0.07. Importantly, the levels of radioactivity measured in cerebellum with the active and inactive enantiomers were superimposable.

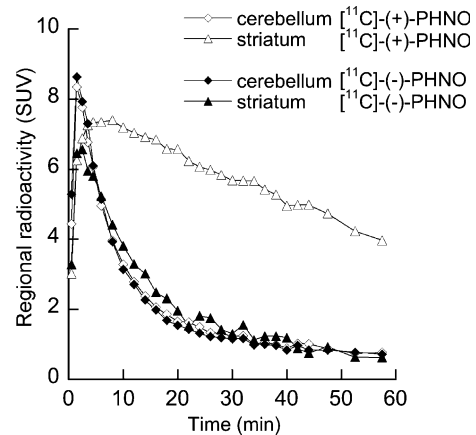


Fig. 2 Comparison of the time–activity curves obtained in the striatum and cerebellum of the same animal following injection of either [^{11}C]-(+)-PHNO or [^{11}C]-(-)-PHNO. Note that there was no preferential uptake of the inactive enantiomer, [^{11}C]-(-)-PHNO, in striatum.

Comparison of [^{11}C]-(+)-PHNO and [^{11}C]-(-)-NPA *in vivo* binding kinetics in the cat brain

Two cats were sequentially examined, at least 4 weeks apart, with [^{11}C]-(+)-PHNO and [^{11}C]-(-)-NPA. Figure 3 shows a comparison of the time–activity curves obtained at baseline in one of the two cats. While the levels of radioactivity measured in cerebellum with the two radioligands were similar, [^{11}C]-(+)-PHNO binding in striatum was higher than

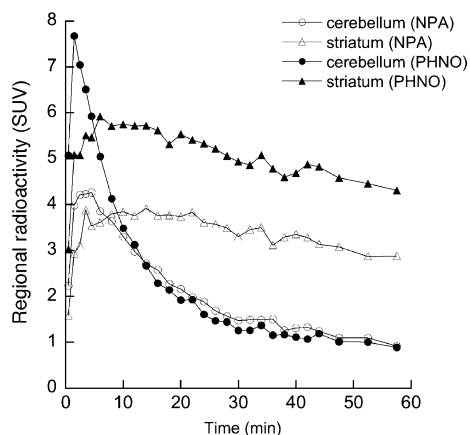


Fig. 3 Comparison of the time–activity curves obtained in the striatum and cerebellum of the same animal following injection of either [¹¹C]-(+)-PHNO or [¹¹C]-(-)-NPA. Note that [¹¹C]-(+)-PHNO uptake in striatum was substantially higher than that obtained with [¹¹C]-(-)-NPA.

that of [¹¹C]-(-)-NPA in the two cats examined. In both cats, striatal BP values were higher using [¹¹C]-(+)-PHNO (3.42 and 3.93) than using [¹¹C]-(-)-NPA (1.59 and 1.39).

Effect of d-amphetamine on [¹¹C]-(+)-PHNO, [¹¹C]-(-)-PHNO and [¹¹C]-(-)-NPA bindings

As exemplified in Fig. 4(a), a single intravenous dose of 2 mg/kg d-amphetamine induced marked reductions of [¹¹C]-(+)-PHNO binding in striatum, but also in cerebellum, when compared with baseline. In this specific animal, [¹¹C]-(+)-PHNO BP was reduced by 88% following d-amphetamine administration; this reduction was due to concomitant 84% and 45% decreases in striatal and cerebellar radioactivity levels, respectively, as measured 31–60 min post-radioligand injection. In stark contrast, no significant change in cerebellar radioactivity levels was observed with [¹¹C]raclopride following administration of the same dose of d-amphetamine (data not shown). To obtain further insight into the mechanism

underlying this decrease in cerebellar [¹¹C]-(+)-PHNO uptake after d-amphetamine, the same animal was scanned at baseline and after 2 mg/kg d-amphetamine using the inactive enantiomer [¹¹C]-(-)-PHNO. As observed with [¹¹C]-(+)-PHNO, d-amphetamine administration induced a marked reduction of [¹¹C]-(-)-PHNO accumulation in brain, including cerebellum, when compared with baseline (Fig. 4b). Importantly, the levels of radioactivity measured in cerebellum with the active and inactive enantiomers were superimposable both at baseline conditions and after the administration of d-amphetamine. Similarly to the observation with [¹¹C]-(+)-PHNO, a 2 mg/kg dose of amphetamine induced marked reductions of [¹¹C]-(-)-NPA binding in both striatum and cerebellum (Fig. 4c). However, the DA-releasing effect of the drug appeared to have less impact on [¹¹C]-(-)-NPA than on [¹¹C]-(+)-PHNO binding, as [¹¹C]-(-)-NPA BP was reduced by ‘only’ 62% following amphetamine administration.

To assess the effect of d-amphetamine on the kinetics of [¹¹C]-(+)- and [¹¹C]-(-)-PHNO in cerebellum, the areas under the time–activity curve (AUC_{0–60min}) obtained in this structure at baseline and after d-amphetamine were compared. The cerebellar AUC_{0–60min} for [¹¹C]-(+)-PHNO was 116 and 68 SUV.min and were at baseline and after d-amphetamine, respectively, comparable with those calculated for [¹¹C]-(-)-PHNO (114 and 64 SUV.min at baseline and after d-amphetamine, respectively). The above results clearly show that d-amphetamine similarly altered the pharmacokinetics of both [¹¹C]-(+)- and [¹¹C]-(-)-PHNO in cerebellum.

To evaluate the time-course of d-amphetamine effect on [¹¹C]-(+)-PHNO binding, the same cat was examined at 20 min, 1 h and 3.5 h post-amphetamine (Fig. 5). [¹¹C]-(+)-PHNO binding kinetics in striatum were still altered at 1 h and at 3.5 h post-amphetamine, with a higher peak uptake and a faster wash-out of radioactivity compared with baseline. Cerebellar AUC_{s0–60min} were still decreased to 83 and 74 SUV.min at 1 h and at 3.5 h post-amphetamine,

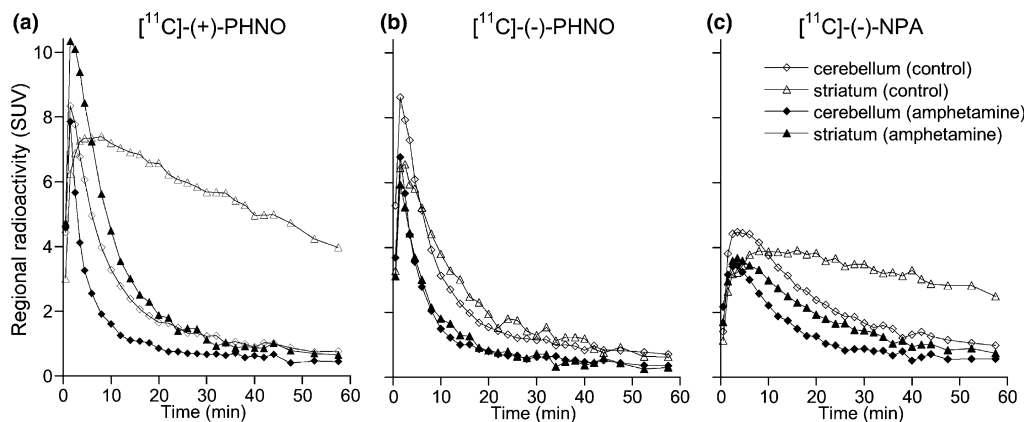


Fig. 4 Effect of a single 2 mg/kg i.v. dose of d-amphetamine on the striatal and cerebellar binding kinetics of (a) [¹¹C]-(+)-PHNO, (b) [¹¹C]-(-)-PHNO and (c) [¹¹C]-(-)-NPA. Note that all three radioligands showed a decreased uptake in cerebellum following d-amphetamine administration.

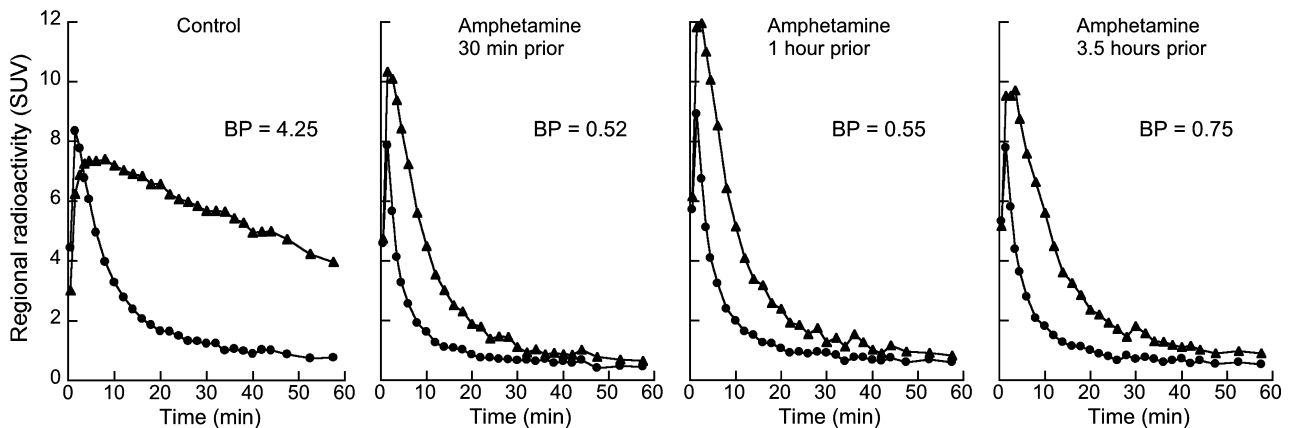


Fig. 5 Time-course of the effect of d-amphetamine on [^{11}C]-(+)-PHNO binding in striatum (closed triangles) and cerebellum (closed circles). [^{11}C]-(+)-PHNO binding kinetics and BPs were obtained in the same animal at 30 min, 1 h and 3.5 h following a single 2 mg/kg i.v. dose of d-amphetamine.

respectively, indicating a long-lasting alteration in [^{11}C]-(+)-PHNO kinetics in brain. [^{11}C]-(+)-PHNO BP was reduced, respectively, by 87% and 82% at 1 h and 3.5 h after the drug, compared with baseline (Fig. 5).

Dose-effect of d-amphetamine on [^{11}C]-(+)-PHNO and [^{11}C]raclopride binding

Doses of radioligand injected

The mean dose and mean mass of [^{11}C]-(+)-PHNO injected at baseline conditions (2.33 ± 0.15 mCi and 0.62 ± 0.20 μg , respectively) were not significantly different from those injected after d-amphetamine administration (2.31 ± 0.16 mCi and 0.60 ± 0.33 μg , respectively; RM ANOVA, $p > 0.05$). Similarly, the mean dose and mean mass of [^{11}C]raclopride injected at baseline conditions (2.30 ± 0.13 mCi and 1.29 ± 0.65 μg , respectively) were not significantly different from those injected after d-amphetamine administration (2.31 ± 0.17 mCi and 1.34 ± 0.53 μg , respectively; RM ANOVA, $p > 0.05$).

Physiological parameters

At baseline conditions, the mean heart rate and mean ETCO_2 measured during the [^{11}C]-(+)-PHNO scans (114 ± 9 beats/min and 30 ± 2 mmHg, respectively) were not significantly different from those measured during the [^{11}C]raclopride scans (109 ± 11 beats/min and 30 ± 3 mmHg, respectively; RM ANOVA, $p = 0.91$ for heart rate and $p = 0.66$ for ETCO_2). Significant elevations in both the heart rate and ETCO_2 were monitored following d-amphetamine administration when compared with baseline, with a significant dose effect for each radioligand (RM ANOVA, $p < 0.001$ for each radioligand and each parameter). The maximal effect was observed at the highest d-amphetamine dose (i.e. 2 mg/kg) for which heart rate increased at 197 ± 3 beats/min and 196 ± 17 beats/min, and ETCO_2 increased at 37 ± 7 mmHg

and 35 ± 8 mmHg, for [^{11}C]-(+)-PHNO and [^{11}C]raclopride, respectively. Under d-amphetamine conditions, no significant difference was observed in the mean heart rate and mean ETCO_2 between the two radioligands (RM ANOVA, $p = 0.54$ for heart rate and $p = 0.53$ for ETCO_2).

Effect of d-amphetamine on radioligand BPs

At baseline conditions, [^{11}C]-(+)-PHNO BP (4.01 ± 0.66 ; $n = 7$) was not significantly different from that measured with [^{11}C]raclopride (3.89 ± 0.44 ; $n = 7$; RM ANOVA, $p = 0.56$; Table 1). d-Amphetamine administration induced significant reductions in [^{11}C]-(+)-PHNO BP when compared with baseline values (RM ANOVA, $p = 0.005$), with a significant dose-effect (RM ANOVA; $p = 0.0001$; Table 1). Similarly, d-amphetamine administration also induced significant reductions in [^{11}C]raclopride BP when compared with baseline (RM ANOVA; $p = 0.002$), with a significant dose-effect (RM ANOVA; $p = 0.0003$; Table 1).

Comparison of the effect of d-amphetamine on both [^{11}C]-(+)-PHNO and [^{11}C]raclopride binding showed that, for all doses used, [^{11}C]-(+)-PHNO was more sensitive to the dopamine releasing effect of the drug (Fig. 6). An omnibus test including both radioligands and all d-amphetamine doses, with D_2 occupancy as the dependent variable, was significant (RM ANOVA, $p = 0.0006$). Post-hoc analysis confirmed that d-amphetamine-released DA induced significantly higher D_2 occupancies when measured with [^{11}C]-(+)-PHNO than when measured with [^{11}C]raclopride (RM ANOVA, $p = 0.002$), with a significant effect of the dose (RM ANOVA, $p = 0.03$). The EDS_{50} of d-amphetamine for inhibiting [^{11}C]-(+)-PHNO and [^{11}C]raclopride striatal bindings were 0.27 mg/kg and 0.39 mg/kg, respectively. The hyperbolic function used to fit the dose-effect data gave maximal occupancy values of 96% for [^{11}C]-(+)-PHNO and of 68% for [^{11}C]raclopride (Fig. 6).

Table 1 Effect of d-amphetamine on [¹¹C]-(+)-PHNO and [¹¹C]raclopride BPs

Dose (mg/kg)	Cat	[¹¹ C]-(+)-PHNO BP			[¹¹ C]raclopride BP		
		Baseline	Post-amphetamine	Occupancy (%)	Baseline	Post-amphetamine	Occupancy (%)
0.1	A	4.13	2.78	32.8	3.78	3.24	14.3
	B	3.30	2.98	9.6	3.40	3.01	11.5
0.5	C	3.93	1.47	62.4	4.40	2.70	38.8
	D	3.53	0.99	71.8	4.11	2.54	39.9
2.0	E	5.31	1.11	79.2	4.34	1.60	63.2
	C	3.63	0.66	81.8	3.26	1.32	59.4
	D	4.24	0.52	87.7	3.97	2.07	47.8

BP corresponds to the binding potential of the radioligand as calculated using the ratio method and data acquired from 31 to 60 min post-radioligand injection. D-amphetamine was injected intravenously, 20–30 min prior to radioligand injection.

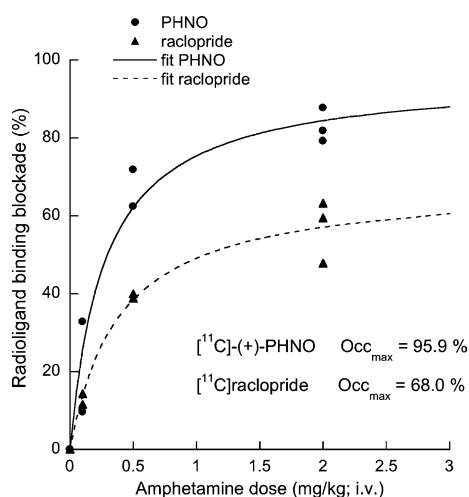


Fig. 6 Relationship between the i.v. dose of d-amphetamine injected and D₂ occupancies measured in the striatum using [¹¹C]-(+)-PHNO and [¹¹C]raclopride. For each radioligand, the symbols correspond to the experimental measured values and the line corresponds to the hyperbolic regression fit to the data. Occ_{max} is the maximal striatal D₂ receptor occupancy (%) induced by d-amphetamine and was derived from the non-linear regression fit to the data.

Dose–effect of haloperidol on [¹¹C]-(+)-PHNO and [¹¹C]raclopride binding

At baseline conditions, [¹¹C]-(+)-PHNO BP (4.29; *n* = 5) was not significantly different from that measured with [¹¹C]raclopride (3.76; *n* = 3; ANOVA, *p* = 0.31; Table 2). Haloperidol administration induced significant reductions in both [¹¹C]-(+)-PHNO and [¹¹C]raclopride BP when compared with baseline values (RM ANOVA, *p* = 0.001 and *p* = 0.04 for [¹¹C]-(+)-PHNO and [¹¹C]raclopride, respectively). An omnibus test including both radioligands and all haloperidol doses, with D₂ occupancy as the dependent variable, was significant (ANOVA, *p* = 0.002). Post-hoc analysis showed that haloperidol-induced D₂ occupancies measured with [¹¹C]-(+)-PHNO were not statistically different from

those measured with [¹¹C]raclopride (ANOVA, *p* = 0.20), with a significant dose–effect (ANOVA, *p* < 0.001). The ED₅₀ of haloperidol for inhibiting [¹¹C]-(+)-PHNO and [¹¹C]raclopride striatal bindings were 28 μg/kg and 19 μg/kg, respectively. The hyperbolic function used to fit the dose–effect data gave maximal occupancy values of 99.6% for [¹¹C]-(+)-PHNO and 97.4% for [¹¹C]raclopride.

Comparison of [¹¹C]raclopride and [¹¹C]-(+)-PHNO binding parameters

In the two cats tested (Figs 7a and b), injection of [¹¹C]-(+)-PHNO at low SR induced a marked reduction of radioactivity levels in striatum, but no detectable changes in cerebellum, when compared with data obtained with the high SR injection. Similar results were obtained with [¹¹C]raclopride (data not shown). These data indicate that [¹¹C]-(+)-PHNO binding in striatum is saturable and suggest that cerebellum is devoid of [¹¹C]-(+)-PHNO specific binding sites.

In the two cats tested, there was no detectable difference in the B_{max} or K'_D values obtained with [¹¹C]-(+)-PHNO when compared with those obtained with [¹¹C]raclopride (Figs 7c and d). In cat C, the B_{max} and K'_D obtained with [¹¹C]raclopride were 30.6 pmol/mL and 10.5 nmol/L, respectively, while B_{max} and K'_D values of 29.6 pmol/mL and 10.3 nmol/L were obtained with [¹¹C]-(+)-PHNO, respectively. In cat E, the B_{max} and K'_D obtained with [¹¹C]raclopride were 33.4 pmol/mL and 10.2 nmol/L with [¹¹C]raclopride, respectively, while B_{max} and K'_D values of 32.9 pmol/mL and 10.1 nmol/L were obtained with [¹¹C]-(+)-PHNO. The B_{max} and K'_D values obtained with [¹¹C]raclopride in this study were comparable with those previously reported in the same species using a similar experimental procedure (Ginovart *et al.* 2002, 2004a).

Discussion

This study demonstrates the suitability of [¹¹C]-(+)-PHNO as an agonist radioligand for *in vivo* PET study of the DA D₂

Dose (mg/kg)	Cat	$[^{11}\text{C}]\text{-}(+)\text{-PHNO BP}$			$[^{11}\text{C}]\text{raclopride BP}$		
		Baseline	Post-haloperidol	Occupancy (%)	Baseline	Post-haloperidol	Occupancy (%)
0.002	B	3.42	2.41	32.7	3.79	2.19	42.2
	D	3.53	2.27	35.7	—	—	—
0.005	C	4.31	0.93	78.5	3.71	0.74	80.0
0.2	E	5.14	0.52	89.8	—	—	—
0.5	E	5.0	0.3	93.5	4.2	0.17	95.9

Table 2 Effect of haloperidol on $[^{11}\text{C}]\text{-}(+)\text{-PHNO}$ and $[^{11}\text{C}]\text{raclopride}$ BPs

BP corresponds to the binding potential of the radioligand as calculated using the ratio method and data acquired from 31 to 60 min post-radioligand injection. Haloperidol was injected intravenously, 1 h prior to radioligand injection.

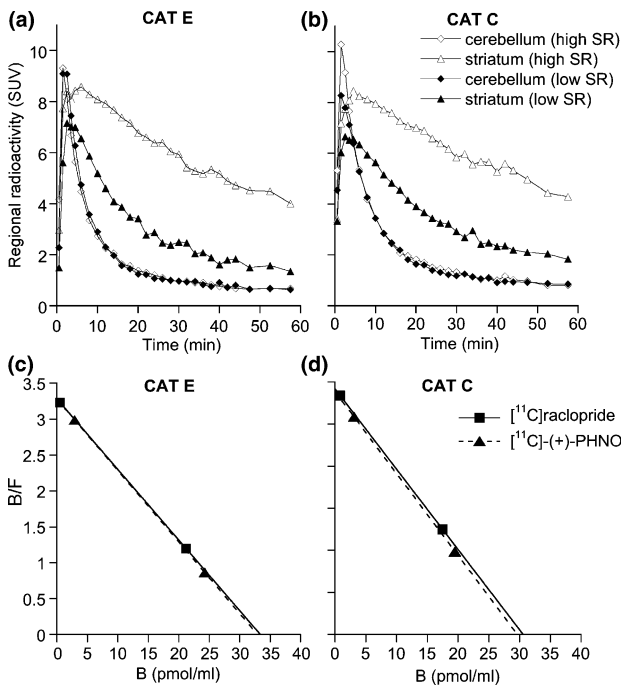


Fig. 7 (a, b) The time–activity curves obtained in striatum and cerebellum of two cats following injection of $[^{11}\text{C}]\text{-}(+)\text{-PHNO}$ at high (open symbols) and at low (closed symbols) specific radioactivity (SR). Note that although a substantial inhibition of $[^{11}\text{C}]\text{-}(+)\text{-PHNO}$ binding was observed in striatum in the low SR experiment, no detectable change was observed in cerebellum. (c, d) Scatchard plots obtained for $[^{11}\text{C}]\text{-}(+)\text{-PHNO}$ and $[^{11}\text{C}]\text{raclopride}$ binding to D_2 receptors in the striatum of the same two cats. Note that in these two cats, the B_{max} and K_{D} obtained with both radioligands were almost identical.

receptor. The *in vivo* distribution of $[^{11}\text{C}]\text{-}(+)\text{-PHNO}$ binding was consistent with the known regional distribution of D_2/D_3 receptors in the cat brain *in vitro* (Richfield *et al.* 1987). The highest uptake of radioactivity was observed in striatum, while low levels of radioactivity were observed in cerebellum, as in all other parts of the brain. $[^{11}\text{C}]\text{-}(+)\text{-PHNO}$ binding in striatum was reduced by up to 94% following pre-treatment with raclopride and haloperidol, indicating that the

vast majority of $[^{11}\text{C}]\text{-}(+)\text{-PHNO}$ binding in this structure represents specific binding to D_2 receptors. Radioactivity levels in cerebellum, a brain region relatively devoid of D_2 receptor sites, was unaffected by these pre-treatments, indicating that cerebellar $[^{11}\text{C}]\text{-}(+)\text{-PHNO}$ binding likely represents free and non-specific binding. Although *in vitro* data showed a marked affinity of $(+)\text{-PHNO}$ for D_3 receptors (Freedman *et al.* 1994; van Vliet *et al.* 2000), pre-treatment with the potent and selective D_3 antagonist, SB-277011 (Stemp *et al.* 2000), did not affect $[^{11}\text{C}]\text{-}(+)\text{-PHNO}$ binding in striatum and cerebellar cortex. These results are understandable as the amounts of D_3 receptor in dorsal striatum is very low when compared with D_2 receptors (Levesque *et al.* 1992; Landwehrmeyer *et al.* 1993), and binding of $[^{11}\text{C}]\text{-}(+)\text{-PHNO}$ to D_3 receptors in this structure would thus represent a very small proportion of the overall signal. In addition, although high levels of D_3 receptors have been reported in lobules 9 and 10 of cerebellum in the rat brain, the cerebellar cortex has undetectable levels of D_3 receptor binding (Levesque *et al.* 1992; Stanwood *et al.* 2000) and showed no specific (i.e. displaceable) binding of $[^{11}\text{C}]\text{-}(+)\text{-PHNO}$.

The binding of $[^{11}\text{C}]\text{-}(+)\text{-PHNO}$ was found to be stereoselective, as the $[^{11}\text{C}]\text{-}(-)\text{-enantiomer}$ showed rapid brain clearance and no selective retention in any regions of the brain. This result is consistent with previous data showing that, *in vitro*, $(-)\text{-PHNO}$ has an over 10 000-fold lower affinity for the D_2 receptor than the active $(+)\text{-enantiomer}$ (Seeman *et al.* 1993) and that, *in vivo*, the efficacy of PHNO for alleviating motor deficits in parkinsonian monkeys is stereoselective (Goulet and Madras 2000). Perhaps as important was the observation that radioactivity levels measured in cerebellum with both the active and inactive enantiomers were superimposable, supporting the assertion that $[^{11}\text{C}]\text{-}(+)\text{-PHNO}$ binding in cerebellum likely represents free and non-specific binding. It thus seems that $[^{11}\text{C}]\text{-}(+)\text{-}$ and $[^{11}\text{C}]\text{-}(-)\text{-PHNO}$ have a high and low affinity for the target receptor, respectively, but the same non-target binding profile. Taken together, these data indicate that $[^{11}\text{C}]\text{-}(+)\text{-PHNO}$ showed the pharmacology expected for a specific *in vivo* D_2 receptor radioligand.

As observed in rats (Wilson *et al.* 2005), [¹¹C]-(+)-PHNO displayed a higher specific to non-specific ratio than [¹¹C]-(-)-NPA in cats, a result consistent with the higher affinity of (+)-PHNO for D₂ receptors than (-)-NPA (Seeman *et al.* 1993). In the two cats examined, striatum/cerebellum ratios of 4.4 and 4.9 were obtained with [¹¹C]-(+)-PHNO, while ratios of 2.4 and 2.6 were obtained with [¹¹C]-(-)-NPA, using data obtained between 31 and 60 min post-injection. This latter finding agrees with the striatum/cerebellum ratio of 2.8 obtained with [¹¹C]-(-)-NPA in baboon at 45 min post-injection (Hwang *et al.* 2000). Our results thus suggest that [¹¹C]-(+)-PHNO may be superior to [¹¹C]-(-)-NPA for PET imaging of the D₂-high.

Pre-treatment with d-amphetamine induced a marked reduction of [¹¹C]-(+)-PHNO binding in both the striatum and cerebellum. While the decreased [¹¹C]-(+)-PHNO binding in striatum was anticipated as the result of an increased competition with endogenous DA, the reduction in cerebellum was rather unexpected and difficult to understand. It is noteworthy that such an unforeseen effect of amphetamine in cerebellum has also been reported for [¹¹C]-(-)-NPA in baboon (Narendran *et al.* 2004) and in cat (present study). These results raise questions about the mechanism by which amphetamine might alter agonist non-specific binding in brain. Indeed, several findings tend to rule out the presence of specific binding sites in cerebellum as an explanation for the observed decrease in [¹¹C]-(+)-PHNO binding in this structure following d-amphetamine. First, D₁, D₂ or D₃ receptor blockade achieved by pre-treatment with specific antagonists did not modify [¹¹C]-(+)-PHNO binding in cerebellum. Importantly, partial saturation of [¹¹C]-(+)-PHNO binding in striatum with unlabeled (+)-PHNO had no detectable effect in cerebellum. Second, cerebellar cortex is known to contain undetectable to extremely low levels of endogenous DA (McIntosh and Westfall 1987; Dethy *et al.* 1997), to have a very modest DA innervation that is restricted to certain lobules of the cerebellar vermis (Melchitzky and Lewis 2000), and to bear negligible amounts of DA transporter sites (Javitch *et al.* 1985; Marcusson and Eriksson 1988) that are required for d-amphetamine-induced DA efflux. Third, the inactive enantiomer radioligand, [¹¹C]-(-)-PHNO, showed decreased binding levels throughout the whole brain following d-amphetamine, a result suggesting an alteration of the free and non-specifically bound radioactivity levels under d-amphetamine conditions. In the light of these data, it is reasonable to assume that the d-amphetamine-induced alterations of [¹¹C]-(+)-PHNO kinetics in cerebellum may be related to a drug-induced alteration of the radioligand's bioavailability in plasma, rather than to an inhibition of specific binding sites. As no data on radioligand metabolism and/or concentration in plasma were obtained in our study, this assumption has not been validated.

Intravenous d-amphetamine at a dose even higher (3.6 mg/kg; i.v.) than the highest dose used in the present study

(2 mg/kg; i.v.) has been reported to produce a transient increase in extracellular striatal DA levels, with a peak response occurring within 2 min after injection and a return to control levels within 2 h (Cho *et al.* 1999). Despite this transient effect of the drug on DA levels, [¹¹C]-(+)-PHNO BP was still reduced at 3.5 h post-amphetamine, thus outlasting the changes in DA levels. Such a long-lasting reduction in radioligand binding following d-amphetamine is also seen with antagonist D₂ radioligands such as [¹¹C]raclopride (Carson *et al.* 2001; Cardenas *et al.* 2004) and [¹²³I]IBZM (Laruelle *et al.* 1997), and has been proposed to reflect a DA-promoted internalization of D₂ receptors (Sun *et al.* 2003; Ginovart *et al.* 2004a). The present study suggests that the binding of agonist radioligands such as [¹¹C]-(+)-PHNO might also be vulnerable to receptor trafficking upon exposure to the endogenous agonist.

In addition to promoting DA release, intravenous d-amphetamine induced significant alterations in physiological parameters, such as increases in heart rate and ET_{CO}₂, as well as an increased peak uptake of [¹¹C]-(+)-PHNO in striatum and cerebellum. These alterations were durable as they were still observed at 1 h and 3.5 h post-amphetamine with [¹¹C]-(+)-PHNO. The increased peak uptake of radioactivity observed after d-amphetamine could be related to an increased cerebral blood flow, as both d-amphetamine (McCulloch and Harper 1977; Russo *et al.* 1991) and hypercapnia (Bryan *et al.* 1988; Williams *et al.* 1991) have been shown to produce large increases in cerebral blood flow.

Radioligand competition paradigms are commonly used to probe DA neurotransmission *in vivo* (for review see Laruelle 2000). In these studies, the amphetamine-evoked increase in DA extracellular levels can be observed using PET by measuring the local displacement of antagonist radioligand such as [¹¹C]raclopride. It seems, however, that there is a ceiling effect to the antagonist displacement such that, even under conditions leading to supraphysiological levels of DA release, only up to 50–60% of [¹¹C]raclopride binding can be displaced. Based on microdialysis data showing that 1.5 mg/kg amphetamine i.v. increases extracellular DA levels by approximately 1900% when compared with baseline values (Laruelle *et al.* 1997), the highest dose of d-amphetamine used in this study (2 mg/kg; i.v.) would be expected to produce a complete occupancy of D₂ receptors. Despite this, only a 56 ± 8% decrease in [¹¹C]raclopride BP was detected in striatum, a result consistent with those we previously reported using the same experimental paradigm *in vivo* in cats (46 ± 5%, Ginovart *et al.* 2004a) and in rats (47%, Ginovart *et al.* 2004b). This relative imperviousness of [¹¹C]raclopride binding to DA manipulations has been related to the inability of antagonists to distinguish the D₂-high from the D₂-low, competition with endogenous DA only occurring at the D₂-high (Laruelle 2000). We found that D₂ receptors labeled with [¹¹C]raclopride showed hyperbolic saturation kinetics with increasing doses of d-amphetamine.

Extrapolation of this hyperbola to infinite d-amphetamine doses gave a theoretical maximal occupancy of [¹¹C]raclopride binding sites by DA of 68% (Fig. 6), therefore suggesting that 68% of the D₂ receptors available for [¹¹C]raclopride binding are in the high-affinity state. This number should, however, be refined, as previous data have shown that at baseline conditions, [¹¹C]raclopride has access to only 65% of the total D₂ receptor population because about 35% of these receptors are already occupied by baseline levels of endogenous DA (Ginovart *et al.* 1997). If these latter receptors are considered to correspond to receptors in the high affinity state, it can be estimated from our data that 79% of the striatal D₂ receptors are configured in the high-affinity state *in vivo*. This estimation is concordant with a number of *in vivo* (Narendran *et al.* 2004, 2005) and *in vitro* (de Vries and Beart 1986; Richfield *et al.* 1986, 1989; Ferre *et al.* 1991; Malmberg and Mohell 1995; Tajuddin and Druse 1996) studies showing that the proportion of D₂-high in striatum ranged between 65 and 80%.

As expected on the basis of its agonist *in vivo* and *in vitro* pharmacological profile, [¹¹C]-(+)-PHNO binding was indeed more vulnerable to the effect of d-amphetamine than [¹¹C]raclopride at every dose, with 2 mg/kg dose of d-amphetamine inducing a 83 ± 4% decrease in [¹¹C]-(+)-PHNO BP but only a 56 ± 8% decrease in [¹¹C]raclopride BP (Table 1). By competing directly for the same high-affinity sites as DA, a full agonist radiotracer at the D₂ receptor should exhibit increased sensitivity to DA levels when compared with antagonists, and should also show full displacement at very high levels of endogenous DA. As reflected in Fig. 6, this prediction was fulfilled, as the maximal occupancy of the [¹¹C]-(+)-PHNO receptor sites by DA obtained by hyperbolic extrapolation was 96%, indicating that virtually all agonist binding sites were displaceable by DA. Together with the similar sensitivity of [¹¹C]-(+)-PHNO and [¹¹C]raclopride to competition with haloperidol, these findings indicate that [¹¹C]-(+)-PHNO binding *in vivo* reflects binding to the D₂-high.

It is noteworthy that a preliminary experiment performed in one cat showed that a 2 mg/kg dose of d-amphetamine induced a 62% decrease in [¹¹C]-(-)-NPA BP, a decrease that is comparable with that reported for [¹¹C]-(-)-NPA in baboon (53 ± 9%; Narendran *et al.* 2004) but substantially lower than the 83 ± 4% decrease in BP obtained with [¹¹C]-(+)-PHNO. These data thus suggest that [¹¹C]-(+)-PHNO may be even more sensitive to DA than [¹¹C]-(-)-NPA.

A head-to-head comparison of the D₂ receptor binding parameters obtained with [¹¹C]-(+)-PHNO and [¹¹C]raclopride showed that both radioligands revealed similar B_{max} values. This result agreed with the report by Ross and Jackson (1989) showing that the B_{max} of [¹¹C]-(-)-NPA equals that of [¹¹C]raclopride in mice striatal homogenates. It disagreed with data by Narendran *et al.* (2005) showing that [¹¹C]-(-)-NPA B_{max} is 79% that of [¹¹C]raclopride *in vivo* in baboon. The reason for this discrepancy is unknown. However, our

data, together with those of Ross and Jackson (1989), suggest that the B_{max} determined with an agonist is similar to that determined with an antagonist, which is counter to the common belief that, based on their pharmacological properties, agonists should only bind to a subset of the overall number of antagonist binding sites. We did not find any plausible explanation to reconcile the experimental evidence with the model of ligand–receptor interaction. Further research is needed to understand more fully the molecular and cellular mechanisms by which [¹¹C]-(+)-PHNO and [¹¹C]raclopride interact with the D₂ receptor *in vivo*.

The use of isoflurane as anesthetic might be viewed as a potential confounding factor of the present study. Several studies indicate that volatile anesthetics such as isoflurane may have a profound effect on brain neurotransmission systems by interfering with the function of G protein. A number of studies on the central nervous system and on preparation of GTP-binding proteins support the view that volatile anesthetics perturb receptor/G protein interaction and prevent the shift to the low-affinity state of G protein-coupled receptors (for review see Rebecchi and Pentylala 2002). However, conflicting data have been reported in this field, suggesting that anesthetics may rather inhibit the high-affinity state of G protein-coupled receptors (Seeman and Kapur 2003). A persistence of the high-affinity D₂ receptor state under isoflurane anesthesia may explain the discrepancy between results obtained in the present study in isoflurane-anesthetized cats and data recently obtained in non-anesthetized rats showing that d-amphetamine used at an i.v. dose of 4 mg/kg induced only a 38% reduction of [¹¹C]-(+)-PHNO binding in striatum (Wilson *et al.* 2005).

In conclusion, this study lends further support to the use of [¹¹C]-(+)-PHNO as an agonist radioligand to image the D₂-high *in vivo* using PET. Its high specificity for the D₂ receptor, high BP values and higher sensitivity for endogenous DA when compared with [¹¹C]raclopride, make it the most promising agonist radioligand developed so far for imaging the D₂-high.

Acknowledgements

The authors thank Armando Garcia, Winston Stableford, Ken Singh, Alvina Ng, Terry Bell and Ted Harris-Brandts for their excellent technical assistance. They also wish to thank CPS Innovations for continued support of the HRRT system at the Center. SK was supported by a CRC Chair in Schizophrenia and Therapeutic Neuroscience. This work was supported by grants from the Canadian Institutes for Health Research (Grants 53330 and 74702).

References

- Bergstrom M., Grahn A. and Langstrom B. (2003) Positron emission tomography microdosing: a new concept with application in tracer and early clinical drug development. *Eur. J. Clin. Pharmacol.* **59**, 357–366.

- Bryan R. M., Jr, Myers C. L. and Page R. B. (1988) Regional neurohypophysial and hypothalamic blood flow in rats during hypercapnia. *Am. J. Physiol.* **255**, R295–R302.
- Cardenas L., Houle S., Kapur S. and Busto U. E. (2004) Oral D-amphetamine causes prolonged displacement of [¹¹C]raclopride as measured by PET. *Synapse* **51**, 27–31.
- Carlsson A. (1987) Perspectives on the discovery of central monoaminergic neurotransmission. *Annu. Rev. Neurosci.* **10**, 19–40.
- Carson R. E., Channing M. A., Vuong B., Watabe H., Herscovitch P. and Eckelman W. C. (2001) Amphetamine-induced dopamine release: duration of action assessed with [¹¹C]raclopride in anesthetized monkeys, in *Physiological Imaging of the Brain with PET* (Gjedde A., ed.), pp. 205–209. Academic Press, San Diego.
- Cho A. K., Melega W. P., Kuczenski R., Segal D. S. and Schmitz D. A. (1999) Caudate-putamen dopamine and stereotypy response profiles after intravenous and subcutaneous amphetamine. *Synapse* **31**, 125–133.
- Defrise M., Kinahan P. E., Townsend D. W., Michel C., Sibomana M. and Newport D. F. (1997) Exact and approximate rebinning algorithms for 3-D PET data. *IEEE Trans. Med. Imag.* **16**, 145–158.
- Dethy S., Manto M., Bastianelli E., Gangji V., Laute M. A., Goldman S. and Hildebrand J. (1997) Cerebellar spongiform degeneration induced by acute lithium intoxication in the rat. *Neurosci. Lett.* **224**, 25–28.
- Ehrin E., Gawell L. H., Högberg T., de Paulis T. and Ström M. P. (1987) Synthesis of [methoxy-³H]- and [methoxy-¹¹C]-labelled raclopride. Specific dopamine-D₂ receptor ligands. *J. Labelled Compd Radiopharm.* **24**, 931–940.
- Farde L., Wiesel F. A., Stone-Elander S., Halldin C., Nordstrom A. L., Hall H. and Sedvall G. (1990) D₂ dopamine receptors in neuroleptic-naïve schizophrenic patients. A positron emission tomography study with [¹¹C]raclopride. *Arch. Gen. Psychiatry* **47**, 213–219.
- Ferre S., von Euler G., Johansson B., Fredholm B. B. and Fuxe K. (1991) Stimulation of high-affinity adenosine A₂ receptors decreases the affinity of dopamine D₂ receptors in rat striatal membranes. *Proc. Natl Acad. Sci. USA* **88**, 7238–7241.
- Finnema S. J., Seneca N., Farde L., Shchukin E., Sovago J., Gulyas B., Wikstrom H. V., Innis R. B., Neumeier J. L. and Halldin C. (2005) A preliminary PET evaluation of the new dopamine D₂ receptor agonist [¹¹C]MNPA in cynomolgus monkey. *Nucl. Med. Biol.* **32**, 353–360.
- Freedman S. B., Patel S., Marwood R., Emms F., Seabrook G. R., Knowles M. R. and McAllister G. (1994) Expression and pharmacological characterization of the human D₃ dopamine receptor. *J. Pharmacol. Exp. Ther.* **268**, 417–426.
- George S. R., Watanabe M. and Seeman P. (1985) Dopamine D₂ receptors in the anterior pituitary: a single population without reciprocal antagonist/agonist states. *J. Neurochem.* **44**, 1168–1177.
- Ginovart N., Farde L., Halldin C. and Swahn C. G. (1997) Effect of reserpine-induced depletion of synaptic dopamine on [¹¹C]raclopride binding to D₂-dopamine receptors in the monkey brain. *Synapse* **25**, 321–325.
- Ginovart N., Hassoun W., Le Cavorsin M., Veyre L., Le Bars D. and Levieil V. (2002) Effects of amphetamine and evoked dopamine release on [¹¹C]raclopride binding in anesthetized cats. *Neuropsychopharmacology* **27**, 72–84.
- Ginovart N., Wilson A. A., Houle S. and Kapur S. (2004a) Amphetamine pretreatment induces a change in both D₂-receptor density and apparent affinity: a [¹¹C]raclopride positron emission tomography study in cats. *Biol. Psychiatry* **55**, 1188–1194.
- Ginovart N., Sun W., Wilson A. A., Houle S. and Kapur S. (2004b) Quantitative validation of an intracerebral beta-sensitive microprobe system to determine *in vivo* drug-induced receptor occupancy using [¹¹C]raclopride in rats. *Synapse* **52**, 89–99.
- Goulet M. and Madras B. K. (2000) D(1) dopamine receptor agonists are more effective in alleviating advanced than mild parkinsonism in 1-methyl-4-phenyl-1,2,3,6-tetrahydropyridine-treated monkeys. *J. Pharmacol. Exp. Ther.* **292**, 714–724.
- Gurevich E. V. and Joyce J. N. (1999) Distribution of dopamine D₃ receptor expressing neurons in the human forebrain: comparison with D₂ receptor expressing neurons. *Neuropsychopharmacology* **20**, 60–80.
- Halldin C., Swahn C. G., Neumeier J. L., Hall H. Y. G. G., Karlsson P. and Farde L. (1992) Preparation of two potent and selective dopamine-D₂ agonists: (R)-[propyl-¹¹C]-2-OH-NPA and (R)-[methyl-¹¹C]-2-OCH₃-NPA. *J. Labelled Compd Radiopharm.* **35**, S265–S266.
- Hietala J., Syvalahti E., Vuorio K., Nagren K., Lehtinen P., Ruotsalainen U., Rakkolainen V., Lehtinen V. and Wegelius U. (1994) Striatal D₂ dopamine receptor characteristics in neuroleptic-naïve schizophrenic patients studied with positron emission tomography. *Arch. Gen. Psychiatry* **51**, 116–123.
- Horn A. S., Hazelhoff B., Dijkstra D., de Vries J. B., Mulder T. B., Timmermans P. and Wynberg H. (1984) The hydroxy-hexahydro-naphthoxazines: a new group of very potent and selective dopamine agonists. *J. Pharm. Pharmacol.* **36**, 639–640.
- Hwang D. R., Kegeles L. S. and Laruelle M. (2000) (-)-N-[(11) C]propyl-norapomorphine: a positron-labeled dopamine agonist for PET imaging of D(2) receptors. *Nucl. Med. Biol.* **27**, 533–539.
- Jasper H. and Ajmone-Marsan C. (1954) *A Stereotaxic Atlas of the Diencephalon of the Cat*. The National Research Council of Canada, Ottawa.
- Javitch J. A., Strittmatter S. M. and Snyder S. H. (1985) Differential visualization of dopamine and norepinephrine uptake sites in rat brain using [³H]mazindol autoradiography. *J. Neurosci.* **5**, 1513–1521.
- Jones J. H., Anderson P. S., Baldwin J. J. *et al.* (1984) Synthesis of 4-substituted 2H-naphth[1,2-b]-1,4-oxazines, a new class of dopamine agonists. *J. Med. Chem.* **27**, 1607–1613.
- Karp J. S., Muehllehner G. and Lewitt R. M. (1988) Constrained Fourier space method for compensation of missing data in emission computed tomography. *IEEE Trans. Med. Imag.* **7**, 21–25.
- Knoess C., Rist J., Michel C. *et al.* (2003) Evaluation of single photon transmission for the HRRT. *IEEE Nucl. Sci. Conf. Rec.* **3**, 1936–1940.
- Landwehrmeyer B., Mengod G. and Palacios J. M. (1993) Differential visualization of dopamine D₂ and D₃ receptor sites in rat brain. A comparative study using *in situ* hybridization histochemistry and ligand binding autoradiography. *Eur. J. Neurosci.* **5**, 145–153.
- Laruelle M. (2000) Imaging synaptic neurotransmission with *in vivo* binding competition techniques: a critical review. *J. Cereb. Blood Flow Metab.* **20**, 423–451.
- Laruelle M., Iyer R. N., al-Tikriti M. S. *et al.* (1997) Microdialysis and SPECT measurements of amphetamine-induced dopamine release in non-human primates. *Synapse* **25**, 1–14.
- Levesque D., Diaz J., Pilon C., Martres M. P., Giros B., Souil E., Schott D., Morgat J. L., Schwartz J. C. and Sokoloff P. (1992) Identification, characterization, and localization of the dopamine D₃ receptor in rat brain using 7-[³H]hydroxy-N,N-di-n-propyl-2-aminotetralin. *Proc. Natl Acad. Sci. USA* **89**, 8155–8159.
- Madras B. K., Fahey M. A., Canfield D. R. and Spelman R. D. (1988) D₁ and D₂ dopamine receptors in caudate-putamen of non-human primates (*Macaca fascicularis*). *J. Neurochem.* **51**, 934–943.

- Malmberg A. and Mohell N. (1995) Characterization of [3H]quinpirole binding to human dopamine D_{2A} and D₃ receptors: effects of ions and guanine nucleotides. *J. Pharmacol. Exp. Ther.* **274**, 790–797.
- Marcusson J. and Eriksson K. (1988) [³H]GBR-12935 binding to dopamine uptake sites in the human brain. *Brain Res.* **457**, 122–129.
- Martin G. E., Williams M., Pettibone D. J., Yarbrough G. G., Clineschmidt B. V. and Jones J. H. (1984) Pharmacologic profile of a novel potent direct-acting dopamine agonist, (+)-4-propyl-9-hydroxynaphthoxazine [(+)-PHNO]. *J. Pharmacol. Exp. Ther.* **230**, 569–576.
- Martin G. E., Williams M., Pettibone D. J., Zrada M. M., Lotti V. J., Taylor D. A. and Jones J. H. (1985) Selectivity of (+)-4-propyl-9-hydroxynaphthoxazine [(+)-PHNO] for dopamine receptors *in vitro* and *in vivo*. *J. Pharmacol. Exp. Ther.* **233**, 395–401.
- Martinot J. L., Peron-Magnan P., Huret J. D. *et al.* (1990) Striatal D₂ dopaminergic receptors assessed with positron emission tomography and [⁷⁶Br]bromospiperone in untreated schizophrenic patients. *Am. J. Psychiatry* **147**, 44–50.
- Martinot J. L., Paillere-Martinot M. L., Loc'h C., Hardy P., Poirier M. F., Mazoyer B., Beaufils B., Maziere B., Allilaire J. F. and Syrota A. (1991) The estimated density of D₂ striatal receptors in schizophrenia. A study with positron emission tomography and ⁷⁶Br-bromolisuride. *Br. J. Psychiatry* **158**, 346–350.
- McCulloch J. and Harper A. M. (1977) Cerebral circulatory and metabolism changes following amphetamine administration. *Brain Res.* **121**, 196–199.
- McIntosh H. H. and Westfall T. C. (1987) Influence of aging on catecholamine levels, accumulation, and release in F-344 rats. *Neurobiol. Aging* **8**, 233–239.
- Melchitzky D. S. and Lewis D. A. (2000) Tyrosine hydroxylase- and dopamine transporter-immunoreactive axons in the primate cerebellum. Evidence for a lobular- and laminar-specific dopamine innervation. *Neuropsychopharmacology* **22**, 466–472.
- Mukherjee J., Narayanan T. K., Christian B. T., Shi B., Dunigan K. A. and Mantil J. (2000) *In vitro* and *in vivo* evaluation of the binding of the dopamine D₂ receptor agonist (11)C-(R,S)-5-hydroxy-2-(di-n-propylamino)tetrinalin in rodents and non-human primate. *Synapse* **37**, 64–70.
- Mukherjee J., Narayanan T. K., Christian B. T., Shi B. and Yang Z. Y. (2004) Binding characteristics of high-affinity dopamine D₂/D₃ receptor agonists, 11C-PPHT and 11C-ZYY-339 in rodents and imaging in non-human primates by PET. *Synapse* **54**, 83–91.
- Narendran R., Hwang D. R., Slifstein M. *et al.* (2004) *In vivo* vulnerability to competition by endogenous dopamine: comparison of the D₂ receptor agonist radiotracer (-)-N-[¹¹C]propyl-norapomorphine ([¹¹C]NPA) with the D₂ receptor antagonist radiotracer [¹¹C]-raclopride. *Synapse* **52**, 188–208.
- Narendran R., Hwang D. R., Slifstein M., Hwang Y., Huang Y., Ekelund J., Guilin O., Scher E., Martinez D. and Laruelle M. (2005) Measurement of the proportion of D₂ receptors configured in state of high affinity for agonists *in vivo*: a positron emission tomography study using [¹¹C]N-propyl-norapomorphine and [¹¹C]raclopride in baboons. *J. Pharmacol. Exp. Ther.* **315**, 80–90.
- Nobrega J. N. and Seeman P. (1994) Dopamine D₂ receptors mapped in rat brain with [³H](+)-PHNO. *Synapse* **17**, 167–172.
- Nordstrom A. L., Farde L., Eriksson L. and Halldin C. (1995) No elevated D₂ dopamine receptors in neuroleptic-naive schizophrenic patients revealed by positron emission tomography and [¹¹C]N-methylspiperone. *Psychiatry Res.* **61**, 67–83.
- Rebecchi M. J. and Pentylala S. N. (2002) Anaesthetic actions on other targets: protein kinase C and guanine nucleotide-binding proteins. *Br. J. Anaesth.* **89**, 62–78.
- Richfield E. K., Young A. B. and Penney J. B. (1986) Properties of D₂ dopamine receptor autoradiography: high percentage of high-affinity agonist sites and increased nucleotide sensitivity in tissue sections. *Brain Res.* **383**, 121–128.
- Richfield E. K., Young A. B. and Penney J. B. (1987) Comparative distribution of dopamine D-1 and D-2 receptors in the basal ganglia of turtles, pigeons, rats, cats, and monkeys. *J. Comp. Neurol.* **262**, 446–463.
- Richfield E. K., Penney J. B. and Young A. B. (1989) Anatomical and affinity state comparisons between dopamine D₁ and D₂ receptors in the rat central nervous system. *Neuroscience* **30**, 767–777.
- Ross S. B. and Jackson D. M. (1989) Kinetic properties of the *in vivo* accumulation of 3H(-)-N-n-propyl-norapomorphine in mouse brain. *Naunyn-Schmiedeberg's Arch. Pharmacol.* **340**, 13–20.
- Russo K. E., Hall W., Chi O. Z., Sinha A. K. and Weiss H. R. (1991) Effect of amphetamine on cerebral blood flow and capillary perfusion. *Brain Res.* **542**, 43–48.
- Seeman P. and Kapur S. (2003) Anesthetics inhibit high-affinity states of dopamine D₂ and other G-linked receptors. *Synapse* **50**, 35–40.
- Seeman P. and Ulpian C. (1988) Dopamine D₁ and D₂ receptor selectivities of agonists and antagonists. *Adv. Exp. Med. Biol.* **235**, 55–63.
- Seeman P., Ulpian C., Larsen R. D. and Anderson P. S. (1993) Dopamine receptors labelled by PHNO. *Synapse* **14**, 254–262.
- Shi B., Narayanan T. K., Yang Z. Y., Christian B. T. and Mukherjee J. (1999) Radiosynthesis and *in vitro* evaluation of 2-(N-alkyl-N-1'-11C-propyl)amino-5-hydroxytetralin analogs as high affinity agonists for dopamine D-2 receptors. *Nucl. Med. Biol.* **26**, 725–735.
- Shi B., Narayanan T. K., Christian B. T., Chattopadhyay S. and Mukherjee J. (2004) Synthesis and biological evaluation of the binding of dopamine D₂/D₃ receptor agonist, (R,S)-5-hydroxy-2-(N-propyl-N-(5'-(18)F-fluoropentyl)aminotetrinalin ((18)F-5-OH-FPPAT) in rodents and non-human primates. *Nucl. Med. Biol.* **31**, 303–311.
- Sibley D. R., De Lean A. and Creese I. (1982) Anterior pituitary dopamine receptors. Demonstration of interconvertible high and low affinity states of the D-2 dopamine receptor. *J. Biol. Chem.* **257**, 6351–6361.
- Stanwood G. D., Artymyshyn R. P., Kung M. P., Kung H. F., Lucki I. and McGonigle P. (2000) Quantitative autoradiographic mapping of rat brain dopamine D₃ binding with [(125)I]7-OH-PIPAT: evidence for the presence of D₃ receptors on dopaminergic and non-dopaminergic cell bodies and terminals. *J. Pharmacol. Exp. Ther.* **295**, 1223–1231.
- Stemp G., Ashmeade T., Branch C. L. *et al.* (2000) Design and synthesis of trans-N-[4-[2-(6-cyano-1,2,3,4-tetrahydroisoquinolin-2-yl)ethyl]cyclohexyl]-4-quinolinecarboxamide (SB-277011): a potent and selective dopamine D(3) receptor antagonist with high oral bioavailability and CNS penetration in the rat. *J. Med. Chem.* **43**, 1878–1885.
- Strange P. G. (1993) New insights into dopamine receptors in the central nervous system. *Neurochem. Int.* **22**, 223–236.
- Suhara T., Okubo Y., Yasuno F. *et al.* (2002) Decreased dopamine D₂ receptor binding in the anterior cingulate cortex in schizophrenia. *Arch. Gen. Psychiatry* **59**, 25–30.
- Sun W., Ginovart N., Ko F., Seeman P. and Kapur S. (2003) *In vivo* evidence for dopamine-mediated internalization of D₂-receptors after amphetamine: differential findings with [3H]raclopride versus [3H]spiperone. *Mol. Pharmacol.* **63**, 456–462.
- Tajuddin N. F. and Druse M. J. (1996) Effects of chronic alcohol consumption and aging on dopamine D₂ receptors in Fischer 344 rats. *Alcohol Clin. Exp. Res.* **20**, 144–151.
- Talvik M., Nordstrom A. L., Olsson H., Halldin C. and Farde L. (2003) Decreased thalamic D₂/D₃ receptor binding in drug-naive patients with schizophrenia: a PET study with [¹¹C]FLB 457. *Int. J. Neuropsychopharmacol.* **6**, 361–370.
- Tuppurainen H., Kuikka J., Viinamaki H., Husso-Saastamoinen M., Bergstrom K. and Tiihonen J. (2003) Extrastriatal dopamine D_{2/3}

- receptor density and distribution in drug-naive schizophrenic patients. *Mol. Psychiatry* **8**, 453–455.
- van Vliet L. A., Rodenhuis N., Dijkstra D. *et al.* (2000) Synthesis and pharmacological evaluation of thiopyran analogues of the dopamine D₃ receptor-selective agonist (4aR,10bR)-(+)-trans-3,4,4a,10b-tetrahydro-4-n-propyl-2H,5H [1]b benzopyrano[4,3-b]-1,4-oxazin-9-ol (PD 128907). *J. Med. Chem.* **43**, 2871–2882.
- de Vries D. J. and Beart P. M. (1986) Role of assay conditions in determining agonist potency at D₂ dopamine receptors in striatal homogenates. *Brain Res.* **387**, 29–35.
- Watson C. C., Newport D., Casey M. E., deKemp R. A., Beanlands R. S. and Schmand M. (1997) Evaluation of simulation-based scatter correction for 3-D PET cardiac imaging. *IEEE Trans. Nucl. Sci.* **44**, 90–97.
- Willeit M., Ginovart N., Kapur S., Houle S., Hussey D., Seeman P. and Wilson A. A. (2006) High-affinity states of human brain dopamine D_{2/3} receptors imaged by the agonist [¹¹C]-(+)-PHNO. *Biol. Psychiatry* **59**, 389–394.
- Williams J. L., Jones S. C., Page R. B. and Bryan R. M., Jr (1991) Vascular responses of choroid plexus during hypercapnia in rats. *Am. J. Physiol.* **260**, R1066–R1070.
- Wilson A. A., Garcia A., Jin L. and Houle S. (2000) Radiotracer synthesis from [(11)C]-iodomethane: a remarkably simple captive solvent method. *Nucl. Med. Biol.* **27**, 529–532.
- Wilson A. A., McCormick P., Kapur S., Willeit M., Garcia A., Hussey D., Houle S., Seeman P. and Ginovart N. (2005) Radiosynthesis and evaluation of [¹¹C]-(+)-4-propyl-3,4,4a,5,6,10b-hexahydro-2H-naphtho[1,2-b][1,4]oxazin-9-ol as a potential radiotracer for *in vivo* imaging of the dopamine D₂ high-affinity state with positron emission tomography. *J. Med. Chem.* **48**, 4153–4160.
- Yasuno F., Suhara T., Okubo Y., Sudo Y., Inoue M., Ichimiya T., Takano A., Nakayama K., Halldin C. and Farde L. (2004) Low dopamine d(2) receptor binding in subregions of the thalamus in schizophrenia. *Am. J. Psychiatry* **161**, 1016–1022.
- Zahniser N. R. and Molinoff P. B. (1978) Effect of guanine nucleotides on striatal dopamine receptors. *Nature* **275**, 453–455.
- Zigmond M. J., Abercrombie E. D., Berger T. W., Grace A. A. and Stricker E. M. (1990) Compensations after lesions of central dopaminergic neurons: some clinical and basic implications. *Trends Neurosci.* **13**, 290–296.
- Zijlstra S., van der Worp H., Wiegman T., Visser G. M., Korf J. and Vaalburg W. (1993a) Synthesis and *in vivo* distribution in the rat of a dopamine agonist: N-[(¹¹C)methyl]norapomorphine. *Nucl. Med. Biol.* **20**, 7–12.
- Zijlstra S., Visser G. M., Korf J. and Vaalburg W. (1993b) Synthesis and *in vivo* distribution in the rat of several fluorine-18 labeled N-fluoroalkylaporphines. *Appl. Radiat. Isot.* **44**, 651–658.